

ChemComm

Accepted Manuscript



This is an *Accepted Manuscript*, which has been through the Royal Society of Chemistry peer review process and has been accepted for publication.

Accepted Manuscripts are published online shortly after acceptance, before technical editing, formatting and proof reading. Using this free service, authors can make their results available to the community, in citable form, before we publish the edited article. We will replace this *Accepted Manuscript* with the edited and formatted *Advance Article* as soon as it is available.

You can find more information about *Accepted Manuscripts* in the [Information for Authors](#).

Please note that technical editing may introduce minor changes to the text and/or graphics, which may alter content. The journal's standard [Terms & Conditions](#) and the [Ethical guidelines](#) still apply. In no event shall the Royal Society of Chemistry be held responsible for any errors or omissions in this *Accepted Manuscript* or any consequences arising from the use of any information it contains.

Cite this: DOI: 10.1039/c0xx00000x

www.rsc.org/xxxxxx

ARTICLE TYPE

pH-sensitive gold nanocluster: preparation and analytical applications for urea, urease, and urease inhibitor

Hao-Hua Deng,^{a,b} Gang-Wei Wu,^{a,c} Zhi-Qiang Zou,^{a,b} Hua-Ping Peng,^{a,b} Ai-Lin Liu,^{a,b} Xin-Hua Lin,^{a,b} Xing-Hua Xia,^d Wei Chen^{*a,b}

Received (in XXX, XXX) Xth XXXXXXXXX 20XX, Accepted Xth XXXXXXXXX 20XX
DOI: 10.1039/b000000x

Herein, we reported for the first time a facile synthetic process of gold nanoclusters (AuNCs) by using N-acetyl-L-cysteine as both reducing agent and protection ligand. Based on the pH stimuli-responsive property of the as-prepared AuNCs, we constructed a pH-sensing platform for the detection of urea, urease, and urease inhibitor.

Due to their unique properties in terms of excellent photophysical properties, facile surface tailorability, easy preparation, and color tenability, fluorescent nanomaterials have become a focus in current nanoscience research. To date, several different types of fluorescent nanomaterials have been developed, including semiconductor quantum dots (QDs),¹ dye-doped nanoparticles,² lanthanide nanoparticles,³ carbon nanodots,⁴ and silica nanoparticles.⁵ Metal nanoclusters (MNCs), comprising few to hundred atoms, have emerged as a new class of luminescent nanomaterials. Their size falls within the range of the Fermi wavelength of conduction electrons and results in size dependent HOMO-LUMO transition and luminescence, thus exhibiting better physical, electrical, optical, and biomedical properties compared to larger cousin metal nanocrystals.⁶ The luminescent MNCs typically have a core-shell structure that consists of two parts: a metal core and a ligand shell.⁷ Different types of ligand shells lead to distinctive differences in physicochemical properties among MNCs, which have made them as appealing functional materials in biosensing and labeling applications.

pH is an important parameter for many biological processes and also a key indicator for disease progression.⁸ For instance, urease (E.C.3.5.1.5) specifically catalyzes the hydrolysis of urea to produce ammonia and carbon dioxide. As it produces ammonia, a basic molecule, urease activity tends to increase the pH of its environment. Bacterial ureases are most often the mode of pathogenesis for many medical conditions such as hepatic encephalopathy/hepatic coma, infection stones, and peptic

^a Department of Pharmaceutical Analysis, Fujian Medical University, Fuzhou 350004, China. E-mail address: chenandhu@163.com (W. Chen).

^b Nano Medical Technology Research Institute, Fujian Medical University, Fuzhou 350004, China

^c Department of Pharmacy, Fujian Provincial Hospital, Fuzhou 350001, China

^d State Key Laboratory of Analytical Chemistry for Life Science, School of Chemistry and Chemical Engineering, Nanjing University, Nanjing 210093, China.

†Electronic Supplementary Information (ESI) available: Experimental details and additional figures. See DOI: 10.1039/b000000x/

ulceration. Therefore, pH-responsive materials serve as powerful tools in the fundamental understanding of medicine for disease diagnosis and therapy. The distinctive structural and photophysical features of nanomaterials open new opportunities for applications of pH probe. Up to now, several kinds of nanomaterials including polymers nanoparticles,⁹ graphene oxide,¹⁰ single-walled carbon nanotube,¹¹ photonic crystals,¹² silica nanoparticles,¹³ QDs,¹⁴ gold nanoparticles,¹⁵ and magnetic nanoparticles¹⁶ have been reported to possess pH stimuli-responsive property. Recently, a few studies have been made in the pH-responsive optical properties of MNCs.¹⁷⁻²⁰ However, applications based on the pH-sensitive MNCs are still in the early stage and the relevant information is extremely rare.

Herein, we reported for the first time the synthesis of water-dispersible, monodispersed AuNCs by a one-pot reaction, in which N-acetyl-L-cysteine (NAC) serves as both reducing agent and stabilizing ligand. Further experiments showed that the NAC-AuNCs exhibit ultrasensitive pH-responsive property in the range of 6.05-6.40. Significantly, the NAC-AuNCs described here are different from and extremely superior to the previously reported nanoscaled pH-probes. The fluorescence of NAC-AuNCs almost totally quench when the pH changes from 6.05 to 6.40, which is dramatically more sensitive ($\Delta\text{pH} < 0.35$ between ON/OFF states) than QDs and other MNCs as pH indicators. Compared to many other pH nanoprobess, the NAC-AuNCs refrain from laborious modification procedures to obtain pH-responsive performance. More importantly, the pH-responsive range of NAC-AuNCs is within the range of physiological dimension, showing potential applications in biological, medical, and pharmaceutical fields.

Fig. 1A presents the absorption spectrum of the NAC-AuNCs. The colorless product missed the characteristic surface plasmon resonance (SPR) peak (~520 nm) of larger gold nanoparticles. The aqueous AuNCs solution emitted strong red fluorescence under UV light irradiation. By fluorescence spectrophotometry (excited at 355 nm), the NAC-AuNCs solution exhibited strong photoluminescence (PL) around 650 nm (Fig. 1B). The emission spectrum did not change with the excitation wavelength varying from 345 to 365 nm (Fig. S1). This indicates that the obtained emission is a real luminescence from the relaxed states and it is not due to scattering effects.²¹ Calculated with quinine sulfate (quantum yield (QY) = 54.0% in 0.1 M H₂SO₄) as a reference, the luminescence QY of the AuNCs was found to be 1.2%. The

fluorescence lifetime of AuNCs collected at PL peak (355 nm) is 765 ns (Fig. S2). The large Stoke's shift and long lifetime are general characteristics of thiol-Au(I)-complexes on the AuNCs surface that displays ligand-metal charge transfer and metal(I)-metal(I) interactions.²² Notably, the NAC-AuNCs have amazing performance in terms of time-stability, photo-stability, and salt and oxidation resistance (Fig. S3), which is caused by two factors: protective shell formed by NAC around AuNCs and stabilization effect of Au(I) presented on the surface of the gold core.²³

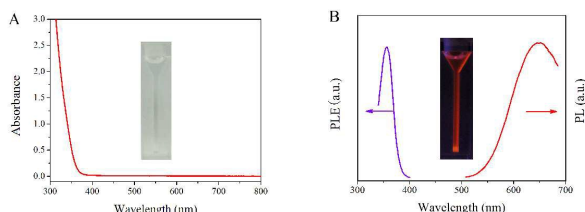


Fig. 1 (A) UV-vis absorption spectrum of the aqueous solution of NAC-AuNCs. The inset shows a photograph of NAC-AuNCs in room light. (B) Fluorescence excitation (blue line, emission at 650 nm) and emission (red line, excitation at 355 nm) spectra of NAC-AuNCs. The inset shows a photograph of NAC-AuNCs under UV light source emitting 365 nm light.

Transmission electron microscopy (TEM) revealed an average diameter of 2.4 ± 0.4 nm for the NAC-AuNCs, as judged from image analysis of 100 individual particles (Fig. S4). The inset high-resolution TEM image shows lattice planes separated by 0.235 nm, corresponding to the (111) lattice spacing of face-centered cubic Au.²⁴ Elemental analysis of NAC-AuNCs determined by energy dispersive X-ray radiation also confirms the presence of Au (Fig. S5). X-ray photoelectron spectroscopy (XPS) measurements were carried out to investigate the electronic structures of the NAC-AuNCs. The Au(4f) XPS spectrum (Fig. S6A) shows the binding energy (BE) of Au(4f_{7/2}) at 84.5 eV, suggesting the existence both of Au(0) and Au(I).²⁵ The spectrum of S(2p) reveals an asymmetric band that can be fitted by two peaks at 162.9 and 164.0 eV, respectively (Fig. S6B). The dominant peak at 162.9 eV is attributed to sulfur atoms of NAC bound to the gold surface. As compared to many studies, it is worth mentioning that the typical band representing the oxidized form of sulfur (at about 167 eV) is absent from the S(2p) region of NAC-AuNCs, further revealing an excellent stability of NAC-AuNCs.^{26, 27} Additionally, C(1S), N(1S), and O(1S) core-level photoemission spectra shown in Fig. S7 originate from the NAC molecules, indicating that the AuNCs are stabilized by NAC. Fourier transform infrared (FTIR) spectra were used to get further insight into the chemical and surface properties of the as-prepared AuNCs. As shown in Fig. S8, the FTIR spectrum of AuNCs exhibits the characteristics of the ligand NAC. The peak at 2547 cm⁻¹ that corresponds to the S-H stretching vibration mode disappeared in NAC-AuNCs,²⁸ indicating that NAC molecule anchor on AuNCs surface through Au-S bonding.

The emission intensity and the wavelength of the MNCs are highly sensitive to the local environments as well as the size and structure of the MNCs, which have made nanoclusters as attractive functional materials in the development of versatile probes. In this work, the PL of NAC-AuNCs at pH values ranging from pH 5.50 to 7.50 was examined and the results were shown in Fig. 2A. The fluorescence intensity of the NAC-AuNCs

changed in a linear fashion over the pH varied from 6.05 to 6.40 (Fig. 2B). In addition, increasing ionic strength could improve the pH-response sensitivity of NAC-AuNCs (Fig. S9). The mechanism of pH-induced fluorescence quenching of NAC-AuNCs was explored. The lifetime of NAC-AuNCs was not changed in aqueous solution with varying pH, proving that the quenching is static (Table S1). XPS was employed to investigate the oxidation state changes of the AuNCs before and after incubating with pH 6.50 buffer. As shown in Fig. S10, the BE for the Au (4f_{7/2}) electrons before and after the addition of pH 6.50 buffer solution is identical, suggesting no change in the oxidation state of NAC-AuNCs. Therefore, the pH-induced PL quenching was not due to the reduction of Au(I) ions on the surface of NAC-AuNCs. UV-vis absorption spectra of NAC-AuNCs in buffer solution with different pH values (6.00-6.75) were recorded (Fig. S11). It can be seen that the background scattering at wavelengths < 450 nm increased obviously with pH increasing from 6.00 to 6.75, which was due to the larger size of the aggregates,²² ruling out the possibility of PL quenching owing to pH-induced aggregation of the NAC-AuNCs. The pH-induced aggregation can be further proved by zeta (ζ) potential (Fig. S12) and hydrodynamic diameter (HDD) measurements (Fig. S13).

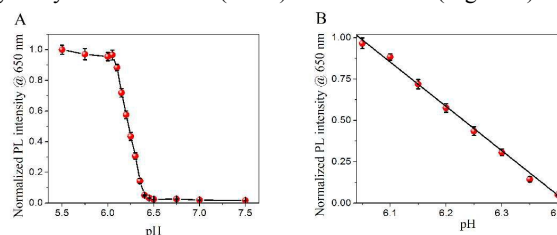


Fig. 2 (A) The plot of the fluorescence intensity of NAC-AuNCs (excitation at 355 nm) recorded at 650 nm (F_{650}) versus pH value. (B) Linear relationship between F_{650} and pH value.

Since the PL intensity of NAC-AuNCs was found to correlate with the acidity (or basicity) of the environment, we expect that NAC-AuNCs can be used as an indicator in monitoring biochemical reactions associated with pH change. For examining the feasibility of such an application, we have designed an analysis system for urea, urease, and urease inhibitor determination. First, the NAC-AuNCs were applied to the detection of urea. The fluorescence intensity decreased with increasing urea concentration (Figure 3A), with a linear response ($r=0.9952$) over urea concentration range of 0.055-0.55 mM (Figure 3A inset). Based on a signal-to-noise ratio (S/N) of 3, the limit detection (LOD) for urea was 0.055 mM. The relative standard deviation (RSD) was 3.6% for the determination of 0.22 mM urea ($n=12$). This approach was comparable and even more efficient for the detection of urea compared to those provided by other nanoprobe.^{29, 30} Fig. S14 revealed the high selectivity of the proposed method for urea detection, which is ascribed to the high specificity of urease toward urea. To validate the practicability of the present assay, we determined the concentration of urea in human urine sample. Table S2 lists the content of urea that we determined in three samples using both our proposed method and the conventional diacetyl monoxime method. The results of t-test and F-test performed at the 95% confidence level demonstrate that the two approaches did not provide significantly different results. Next, we investigated the

application of this method to evaluating urease activity. The fluorescence intensity decreased with increasing the enzyme activity of urease (Fig. 3B), the F_{650} values were linear ($r=0.9939$) with the urease activity within the range from 2.2 to 55 U/L (Fig. 3B inset). The LOD, based on a S/N of 3, was calculated to be 0.55 U/L. The RSD was 3.2% for the detection of 11 U/L urease ($n=12$). To test the feasibility of the method for practical application, we applied it to detect *H. pylori* in human gastric tissue. The results obtained from our established approach were in line with conventional method using bromothymol blue as a pH indicator (Fig. 3C, D), and moreover this assay greatly shortened analyzing time (Fig. S15). Furthermore, the NAC-AuNCs-mediated pH probe was also used to evaluate the inhibition of urease in the presence of small molecule inhibitors. According to previous studies,^{31, 32} cysteamine (Cys) and p-benzoquinone (Ben) were employed as inhibitors. On the basis of the results (Figure 3E, F), the half-maximal inhibition value IC_{50} of Cys and Ben were 2.8 μ M and 11.9 μ M, respectively.

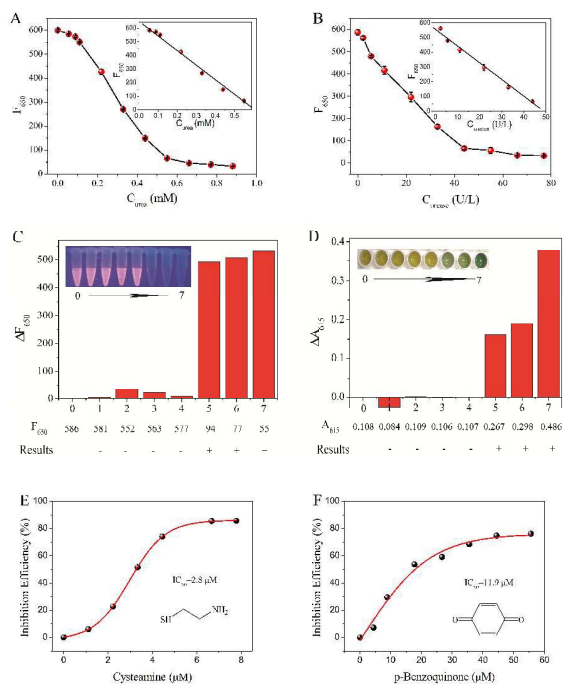


Fig. 3 (A) The plot of F_{650} (excitation at 355 nm) versus the concentration of urea. Inset: linear relationship between F_{650} and the concentration of urea. (B) The plot of F_{650} (excitation at 355 nm) versus the enzyme activity of urease. Inset: linear relationship between F_{650} and the enzyme activity of urease. Results of the developed approach (C) and conventional bromothymol blue method (D) for the detection of *H. pylori* in human gastric tissue. Inhibition efficiency of urease by Cys (E) and Ben (F). The IC_{50} values were obtained from the fitting curve.

In summary, we have demonstrated the NAC-directed synthesis of fluorescent AuNCs. They show ultrasensitive pH-responsive property in the range of 6.05-6.40. On the basis of this property, a simple sensing platform for the detection of urea, urease, and urease inhibitors was developed. Our finding broadens the use of AuNCs in analytical and bioanalytical chemistry. Coupled with their photoluminescence properties, we believe that the NAC-AuNCs would be a promising candidate in the applications in biological, pharmaceutical, industrial fields,

and so on.

This work was supported by the National Natural Science Foundation of China (21175023), the Program for New Century Excellent Talents in University (NCET-12-0618), the Natural Science Foundation of Fujian Province (2012J06019), and the Medical Elite Cultivation Program of Fujian (2013-ZQN-ZD-25). We thank Xin-Xia Fan from Fuzhou University for her assistance in fluorescence lifetime spectrometer.

Notes and references

- A. A. Cordones, M. Scheele, A. P. Alivisatos and S. R. Leone, *J. Am. Chem. Soc.*, 2012, **134**, 18366-18373.
- J. Yan, M. C. Estévez, J. E. Smith, K. Wang, X. He, L. Wang and W. Tan, *Nano Today*, 2007, **2**, 44-50.
- H. Dong, L.-D. Sun and C.-H. Yan, *Nanoscale*, 2013, **5**, 5703-5714.
- S. Zhu, Q. Meng, L. Wang, J. Zhang, Y. Song, H. Jin, K. Zhang, H. Sun, H. Wang and B. Yang, *Angew. Chem. Int. Ed.*, 2013, **125**, 4045-4049.
- H. Ow, D. R. Larson, M. Srivastava, B. A. Baird, W. W. Webb and U. Wiesner, *Nano Lett.*, 2005, **5**, 113-117.
- L. Shang, S. Dong and G. U. Nienhaus, *Nano Today*, 2011, **6**, 401-418.
- X. Yuan, Z. Luo, Y. Yu, Q. Yao and J. Xie, *Chem. Asian J.*, 2013, **8**, 858-871.
- M. Yu, C. Zhou, J. Liu, J. D. Hankins and J. Zheng, *J. Am. Chem. Soc.*, 2011, **133**, 11014-11017.
- D. N. Robinson and N. A. Peppas, *Macromolecules*, 2002, **35**, 3668-3674.
- S. Sun and P. Wu, *J. Mater. Chem.*, 2011, **21**, 4095-4097.
- D. Wang and L. Chen, *Nano Lett.*, 2007, **7**, 1480-1484.
- C. Fenzl, C. Genslein, A. Zöpfl, A. J. Baeumner and T. Hirsch, *J. Mater. Chem. B*, 2015, **3**, 2089-2095.
- G. Li, G. Liu, E. Kang, K. Neoh and X. Yang, *Langmuir*, 2008, **24**, 9050-9055.
- K. Paek, S. Chung, C.-H. Cho and B. J. Kim, *Chem. Commun.*, 2011, **47**, 10272-10274.
- D. Li, Q. He, Y. Cui and J. Li, *Chem. Mater.*, 2007, **19**, 412-417.
- L. Yang, C. Guo, L. Jia, K. Xie, Q. Shou and H. Liu, *Ind. Eng. Chem. Res.*, 2010, **49**, 8518-8525.
- F. Qu, N. B. Li and H. Q. Luo, *Langmuir*, 2013, **29**, 1199-1205.
- X. Jia, X. Yang, J. Li, D. Li and E. Wang, *Chem. Commun.*, 2014, **50**, 237-239.
- P.-C. Chen, J.-Y. Ma, L.-Y. Chen, G.-L. Lin, C.-C. Shih, T.-Y. Lin and H.-T. Chang, *Nanoscale*, 2014, **6**, 3503-3507.
- W. Wang, F. Leng, L. Zhan, Y. Chang, X. X. Yang, J. Lan and C. Z. Huang, *Analyst*, 2014, **139**, 2990-2993.
- L. Shang, R. M. Dörlich, S. Brandholt, R. Schneider, V. Trouillet, M. Bruns, D. Gerthsen and G. U. Nienhaus, *Nanoscale*, 2011, **3**, 2009-2014.
- Z. Luo, X. Yuan, Y. Yu, Q. Zhang, D. T. Leong, J. Y. Lee and J. Xie, *J. Am. Chem. Soc.*, 2012, **134**, 16662-16670.
- C. Wang, Y. Wang, L. Xu, X. Shi, X. Li, X. Xu, H. Sun, B. Yang and Q. Lin, *Small*, 2013, **9**, 413-420.
- C. Wang, Y. Hu, C. M. Lieber and S. Sun, *J. Am. Chem. Soc.*, 2008, **130**, 8902-8903.
- L. Shang, N. Azadfar, F. Stockmar, W. Send, V. Trouillet, M. Bruns, D. Gerthsen and G. U. Nienhaus, *Small*, 2011, **7**, 2614-2620.
- P. L. Xavier, K. Chaudhari, P. K. Verma, S. K. Pal and T. Pradeep, *Nanoscale*, 2010, **2**, 2769-2776.
- Z. Tang, B. Xu, B. Wu, M. W. Germann and G. Wang, *J. Am. Chem. Soc.*, 2010, **132**, 3367-3374.
- Q. Wang, X. Yu, G. Zhan and C. Li, *Biosens. Bioelectron.*, 2014, **54**, 311-316.
- C.-P. Huang, Y.-K. Li and T.-M. Chen, *Biosens. Bioelectron.*, 2007, **22**, 1835-1838.
- L. V. Nair, D. S. Philips, R. S. Jayasree and A. Ajayaghosh, *Small*, 2013, **9**, 2673-2677.

-
31. M. J. Todd and R. Hausinger, *J. Biolog. Chem.*, 1989, **264**, 15835-15842.
 32. M. Kot, *J. Enzym. Inhib. Med. Chem.*, 2006, **21**, 697-701.